

Transmission Phase of a Singly Occupied Quantum Dot in the Kondo Regime

M. Zaffalon, Aavek Bid, M. Heiblum, D. Mahalu, and V. Umansky

*Braun Center for Submicron Research, Department of Condensed Matter Physics, Weizmann Institute of Science,
76100 Rehovot, Israel*

(Received 7 November 2007; published 2 June 2008)

We report on the phase measurements on a quantum dot containing a single electron in the Kondo regime. Transport takes place through a single orbital state. Although the conductance is far from the unitary limit, we measure directly, for the first time, a transmission phase as theoretically predicted of $\pi/2$. As the dot's coupling to the leads is decreased, with the dot entering the Coulomb blockade regime, the phase reaches a value of π . Temperature shows little effect on the phase behavior in the range 30–600 mK, even though both the two-terminal conductance and amplitude of the Aharonov-Bohm oscillations are strongly affected. These results also suggest that previous phase measurements involved transport through more than a single level.

DOI: [10.1103/PhysRevLett.100.226601](https://doi.org/10.1103/PhysRevLett.100.226601)

PACS numbers: 72.15.Qm, 73.23.Hk, 85.35.Ds, 85.35.Gv

What is the transmission amplitude of an electron scattered off a Kondo cloud? The Kondo effect, first observed in bulk metals doped with a small concentration of magnetic impurities [1], manifests itself as an enhancement of the scattering rate below the Kondo temperature T_K (the many-body energy scale of the Kondo correlated system), below which the impurity spin is totally screened by the conduction electrons in the host metal.

The Kondo effect was predicted [2–4] and experimentally observed [5–7] in a quantum dot (QD), which acts as a single magnetic impurity with tunable coupling to the screening electrons in the leads. In fact, a QD [8,9], a small confined region connected by two tunnel barriers to electron reservoirs, is characterized by an on-site charging energy U owing to its small capacitance, by level quantization ϵ because of lateral confinement, and by homogeneous level broadening due to finite coupling Γ . In addition, the QD energy levels can be tuned, allowing one to change the QD occupancy $\langle N \rangle$.

The Kondo effect in a QD is easily probed by conductance measurements. Conductance takes place approximately at the charge degeneracy points, involving, say, electrons 0 and 1, when the energy ϵ_0 to add the first electron to the empty dot is $\epsilon_0 \approx 0$ (or when $\epsilon_0 + U \approx 0$, to add a second electron with opposite spin). Away from these points only cotunneling, processes involving two or more simultaneous tunneling events, occur and the conductance is expected to be suppressed. However, when $\langle N \rangle = 1$, the Kondo effect allows for a substantial current flow if $T \lesssim T_K$, reaching a maximum conductance of $G_{\max} = 2e^2/h$, the unitary limit, at $T = 0$. Strictly speaking, the Kondo regime is limited to the parameter region $-U + \Gamma \lesssim \epsilon_0 \lesssim -\Gamma$ [7,10]. If $\Gamma/\Delta\epsilon \lesssim 0.5$, one single orbital state is involved and $T_K(\epsilon_0) = \frac{\sqrt{\Gamma U}}{2} \exp(\frac{\pi\epsilon_0(\epsilon_0+U)}{\Gamma U})$: with this definition $G(T_K) = G_{\max}/2$, with $G_{\max} = 2e^2/h$ if the barriers are symmetric [7].

Whereas the conductance is proportional to the transmission probability through the QD, it discards informa-

tion about the electron transmission phase. At $T = 0$ the conductance G and the transmission phase δ are related by $G = G_{\max} \sin^2 \delta$ [7,11,12], predicting a monotonic phase evolution with a phase rise of $\pi/2$ from $\langle N \rangle = 0$ to $\langle N \rangle = 1$, followed by a constant phase shift in the Kondo valley ($\epsilon_0 = -U/2$), raising to π when the QD is doubly occupied, outside the Kondo region. At finite temperature, the monotonicity disappears, but even at $T \approx 10T_K$, the transmission phase climbs only to 0.7π across the first peak before decreasing to $\pi/2$ in the Kondo valley [13]. At $T \gg T_K$, Kondo correlations are negligible and the well known result for the Coulomb regime is expected: a π rise across each peak [14,15] and a phase lapse in the conductance valley, with a *total* phase evolution of π . For an arbitrary temperature, the phase can be calculated only by numerical renormalization group [10]: these results, based on the single-level Anderson impurity model, predict a smooth evolution between the Kondo and the Coulomb blockade regime.

Previous measurements of the phase shift by Ji *et al.* [16,17] were obtained using an interferometer with the Kondo dot placed in one of its arms. They found a phase evolution of about 1.5π across the two peaks, both in the nonunitary and in the unitary limit, the two phase evolutions differing only in the presence of a plateau situated at $\delta = \pi$ in the Kondo valley in the nonunitary case. A different approach was taken by Sato *et al.* [18] who studied the resonances induced by a Kondo-dot side coupled to a quantum wire. They deduced a phase shift of $\pi/2$ by analyzing Fano resonances in the conductance.

There is by now vast theoretical evidence (for a summary, see [19]) that the transmission phase depends on the specific properties of the QD's levels that participate in the transport. In this Letter we report on measurements on a QD in which transport takes place through a single level. To ensure this condition, we fabricated a QD, similar to the type described by Ciorga *et al.* [20] in which transport is still substantial when $\langle N \rangle = 1$ electron [21]. This gives

large level spacings, as the *average* level spacing decreases with $1/\sqrt{\langle N \rangle}$.

The determination of the phase evolution is based on the interference between two paths—the two arms of an interferometer—one of which contains the QD [22] and the other being the reference arm, with transmission amplitudes $t_{\text{QD}}^{\text{coh}}(\epsilon_0) = |t_{\text{QD}}^{\text{coh}}(\epsilon_0)|e^{i\varphi_{\text{QD}}(\epsilon_0)}$ and t_{ref} , respectively. In an *open* interferometer [15,16,23], four grounded bases collect the backscattered electrons and only two direct paths from emitter to collector are possible. A weak magnetic field B threading the island adds an Aharonov-Bohm (AB) phase $\varphi_{\text{AB}} = 2\pi\phi/\phi_0$ to the electron, where ϕ is the magnetic flux enclosed by the electron path and $\phi_0 = h/e$ is the flux quantum. The coherent current at the collector is proportional to $|t_{\text{ref}} + t_{\text{QD}}^{\text{coh}}e^{-i\varphi_{\text{AB}}}|^2 = (\text{constant term}) + 2|t_{\text{ref}}||t_{\text{QD}}^{\text{coh}}|\cos(\varphi_{\text{AB}} + \varphi_{\text{QD}} + \phi')$: the former part is weakly B dependent, owing to the Lorentz force, and the latter, $T^{\text{flux}}(\epsilon_0)\cos[\varphi_{\text{AB}} + \varphi_{\text{QD}}(\epsilon_0) + \phi']$, is periodic in the flux quantum; ϕ' is a constant interferometer-dependent phase.

Referring to Fig. 1, the device is fabricated on a two-dimensional electron gas embedded in a AlGaAs/GaAs heterostructure, some 60 nm beneath the surface, with carrier density of $3.3 \times 10^{15} \text{ m}^{-2}$ and mobility of $1.2 \times 10^2 \text{ V/m}^2\text{s}$ at 4.2 K. Two subsequent steps of electron beam lithography are required to pattern the gates and the bridge. The four reflectors can be individually biased in order to focus the electrons from emitter to collector and increase the signal. The reference arm, which can be blocked by the switch gate, carries approximately 10 conducting modes and the arm with the dot about 5. Measurements are performed on one device in a dilution refrigerator with electron temperature of 30 mK. Conductance measurements of the QD are taken with $v_{\text{sd}} = 5 \mu\text{V}$ excitation voltage below 300 mK and $v_{\text{sd}} = 10\text{--}20 \mu\text{V}$ above 300 mK at 250 Hz and the current is measured with an Ithaco 1211 current preamplifier. A second device, measured in a dilution refrigerator with electron temperature of 150 mK, behaved in a quantitative similar manner.

A quantum point contact (QPC) is situated in close proximity to the QD. It detects the average QD occupation,

as the conductance through the QPC is affected by the electrostatic potential of the QD. In order to enhance the sensitivity of the detection, we employ the measuring scheme previously used by Sprinzak *et al.* [24]. Figure 1(b) shows the dot's two-terminal conductance, together with the detector signal, revealing the QD *absolute* occupancy $\langle N \rangle = 0, 1, 2$: a dip in the detector signal appears whenever the QD average occupation changes by one electron.

Two-terminal conductance measurements of the QD are taken between the bases in order to avoid the emitter and collector series resistance. From finite bias scans, we evaluate the charging energy to be $U \approx 3.0 \pm 0.2 \text{ meV}$ and the first excited state for the first electron to be $\Delta\epsilon_1 = 0.80 \pm 0.05 \mu\text{eV}$, whereas for the second peak, the level spacing decreases to $\Delta\epsilon_2 = 0.30 \pm 0.05 \mu\text{eV}$. We then tune the coupling of the QD to the leads so as to maximize the conductance of the first two peaks, with the constraint that the conductance in the $\langle N \rangle = 2$ valley is lower than about $(0.05\text{--}0.1)e^2/h$: failing to do so results in the phase evolution being featureless, probably due to multilevel transport. On the offside, this results in a lower T_K . For the case of Fig. 3 below, with $\Gamma = 180 \mu\text{eV}$ as evaluated from the width of the resonance at finite bias where Kondo correlations are suppressed, the Kondo temperature was estimated to be 1 mK at $\epsilon_0 = -U/2$.

The presence of Kondo correlations is verified by the following characteristics: the peaks' conductance being larger than $G_0 = e^2/h$ and the suppression of the peak conductance by the application of a finite bias [7]. Figure 2(a) shows a series of two-terminal conductance traces of the first two peaks, as a function of the temperature. Differential conductance traces for some plunger voltages are reported in Fig. 2(b) at base temperature: the resonances at finite bias are probably induced by the reflectors.

Once the Kondo-enhanced peaks are identified, we set the emitter and collector QPCs of the interferometer to a conductance of $(2\text{--}3)e^2/h$. We then open the reference arm and measure the ballistic current between emitter and collector with all bases grounded, while a weak magnetic

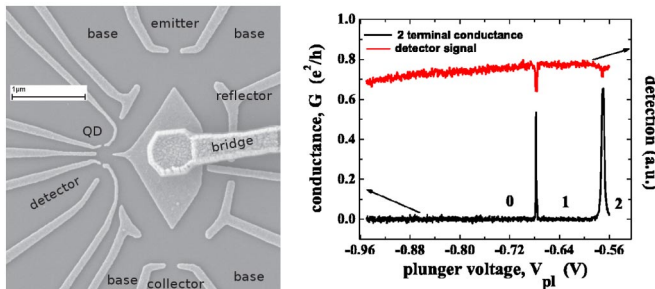


FIG. 1 (color online). SEM micrograph of the device and electron counting. Left: Micrograph of the interferometer with the QD embedded in one arm. Right: Two-terminal conductance of the QD with the last two electrons and the detector signal.

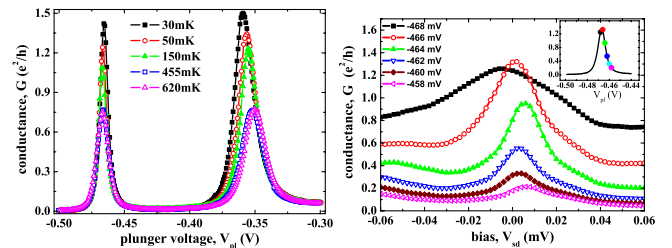


FIG. 2 (color online). Two-terminal conductance: temperature and bias dependence. Left: Temperature dependence of the first two peaks ($\Gamma = 180 \pm 25 \mu\text{eV}$ for the first peak). Right: Two-terminal finite source drain bias scans taken in correspondence to the first peak at plunger biases indicated by the dots on the trace in the inset.

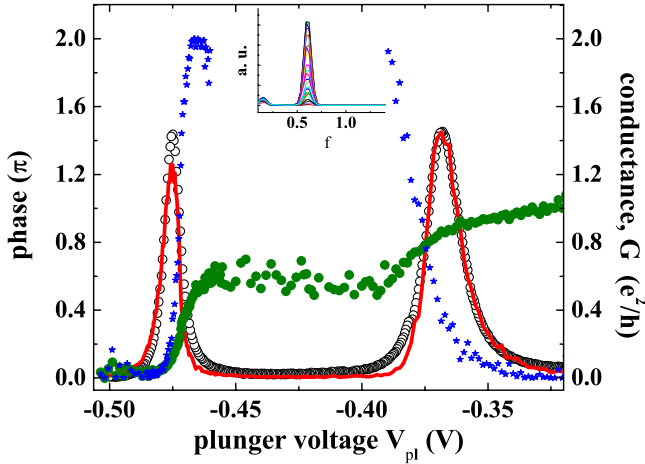


FIG. 3 (color online). Phase evolution in the QD. Two-terminal conductance (open circles), AB amplitude squared, $(T^{\text{flux}})^2$ (full line), and phase of two peaks (full dots). The turquoise stars are calculated from the expression $G = 2e^2/h \sin^2 \delta$. Inset: Amplitude squared of the AB oscillations, showing f_0 the fundamental frequency.

field is swept, in the range of tens of milliTesla. Typically, about 95% of the injected current is lost to the bases. The current at the collector shows AB oscillations with visibility (ratio of the amplitude of the oscillations to the average background) of about 20%. The period $f_0 = 0.61 \text{ mT}^{-1}$ corresponds to an area enclosed by the electron paths of $1.64 \mu\text{m}^2$, comparable to the interferometer area of $1.7 \mu\text{m}^2$.

The amplitude squared $(T^{\text{flux}})^2 \propto |t_{QD}^{\text{coh}}|^2$ of the AB oscillations at the frequency f_0 is plotted in Fig. 3, together with the phase evolution, as determined by Fourier analysis and normalized such that the maximum of $(T^{\text{flux}})^2$ coincides with the maximum of G_{2t} , the line trace in the figure. This is based on the assumption that at $T \ll T_K$ all transport processes are coherent [10,11].

Three features are evident: (a) the phase evolution across the two peaks is π and it seems to saturate at a value of $\approx 0.5\pi$ across the first peak and again $\approx 0.5\pi$ across the second peak, even though for the second peak the condition of single-level transport $\Gamma/\Delta\epsilon_2 \lesssim 0.5$ is not strictly satisfied. In the valley, the coherent current is below the noise level and the phase evolution can barely be followed. This phase behavior is in qualitative agreement with the prediction of Gerland *et al.* [10] for transport through one orbital level and in disagreement with the previous measurement in a similar open interferometer of Ji *et al.* [16]. (b) $(T^{\text{flux}})^2$ closely follows G_{2t} , except in the $\langle N \rangle = 1$ conductance valley: in fact, G_{2t} also includes incoherent processes that do not contribute to the AB oscillations [13,25]. (c) The stars in Fig. 3 are calculated from the relationship $G = G_{\text{max}} \sin^2 \delta$, valid outside the Kondo regime where $T \ll \Gamma/k_B$. Here we set $G_{\text{max}} = 2e^2/h$, as the couplings are approximately equal. It is evident that a different choice of G_{max} would not give a better agreement.

A first conclusion can now be drawn: although the QD exhibits Coulomb blockadelike features (highly suppressed current in the valley) and only energy dependence reveals Kondo correlations, the phase evolution is drastically different to that in the Coulomb regime, proving the extreme sensitivity of the phase to correlations [13].

We now proceed to decrease the QD coupling so as to decrease $T_K(\epsilon_0)$. We expect to see a transition to a π phase shift across each peak in the Coulomb blockade limit. Figure 4 shows such transition of the phase evolution to 0.9π when the first peak width is about $50 \mu\text{eV}$. In contrast to the results reported by Avinun-Kalish *et al.* [15], the phase across the first two peaks is limited to the π rise, indicating transport through the same orbital [19].

The Kondo effect can also be suppressed by raising the temperature: we now proceed to measure the temperature dependence of the phase, in the temperature range 30–600 mK. The measurements are taken in the following way: we tune the peaks at base temperature to have the required width, and scan the two-terminal and multiterminal conductances at different temperatures. A little retuning is sometimes required between one temperature value and the following as a typical phase scan requires approximately 10 hours.

Both G_{2t} and the AB oscillations are strongly affected by temperature: $(T^{\text{flux}})^2$ at the highest temperature is ≈ 30

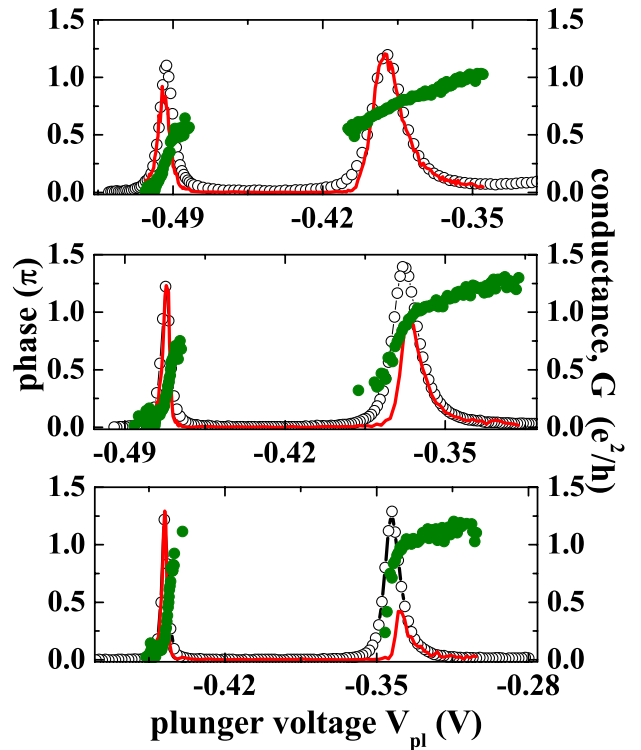


FIG. 4 (color online). Phase evolution for $\Gamma = 180, 110$, and $50 \mu\text{eV}$ at 30 mK. The phase climb across the first peak changes from 0.6π to 0.9π as Γ decreases. $(T^{\text{flux}})^2$ has been normalized to G_{2t} , even though at smaller Γ , the above-mentioned argument ceases to be valid as $T \gtrsim T_K$.

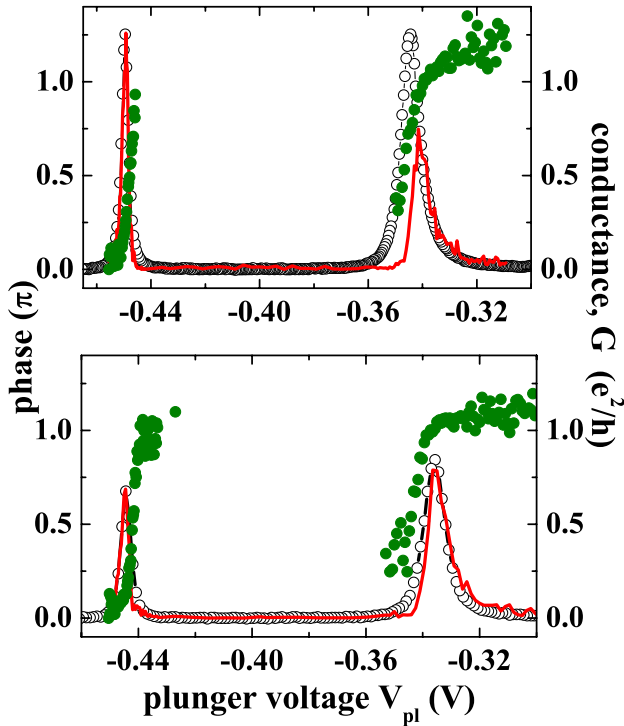


FIG. 5 (color online). Phase evolution as a function of the temperature for the narrowest peak, $\Gamma = 80 \pm 10 \mu\text{eV}$ at base temperature and 300 mK, showing a transition to π phase evolution across each peak.

times smaller than that at base temperature. However, as for the phase, no temperature dependence is observed for the wide peaks ($\Gamma = 180$ and $\Gamma = 110 \mu\text{eV}$), up to 600 mK within the experimental error. For the narrow peak, $\Gamma = 80 \mu\text{eV}$, the phase is 0.8π at base temperature and increases to π at $T = 300$ mK; see Fig. 5. This is consistent with the robustness of the phase evolution pointed out by Silvestrov *et al.* [13]. We believe that the larger discrepancy of shape between the G_{2l} and $(T^{\text{flux}})^2$ for the second peak in Figs. 4 and 5 can be due to two main reasons: (1) an impurity moving close to the quantum dot and (2) the switching of the dominant conducting channel as a function of the plunger voltage in the arm containing the dot.

In conclusion, we have shown that the transmission phase through a QD evolves from a π phase shift in the Coulomb regime to $\approx \pi/2$ in the Kondo and it persists at temperatures up to 5–10 times T_K . A temperature induced change of the phase evolution could only be seen with the smallest coupling. These results provide some more insight into the previously measured phase evolution through a QD. We are in the position to identify three distinct behaviors: (1) $\Gamma \approx k_B T$ gives the Coulomb blockade result π , for the transmission phase; (2) $\Gamma \gtrsim 30k_B T$, the Kondo result of $\pi/2$; (3) $\Gamma \gg \Delta\epsilon$, i.e., multilevel transport [15,23], a π phase rise across each peak.

We acknowledge useful discussions with Yuval Gefen, Keren Michaeli, Peter Silvestrov, Theresa Hecht, Jan

von Delft, Andrei Kretinin, Yaron Bromberg, and especially Yuval Oreg and David Goldhaber-Gordon, and the technical help of Sandra Foletti, Yunchul Chung, Oren Zarchin, and Michal Avinun-Kalish.

-
- [1] A. C. Hewson, *The Kondo Problem to Heavy Fermions* (Cambridge University Press, Cambridge, England, 1997).
 - [2] T. K. Ng and P. A. Lee, Phys. Rev. Lett. **61**, 1768 (1988).
 - [3] L. I. Glazman and M. E. Raikh, JETP Lett. **47**, 452 (1988).
 - [4] Y. Meir and N. S. Wingreen, Phys. Rev. Lett. **70**, 2601 (1993).
 - [5] D. Goldhaber-Gordon, H. Shtrikman, D. Mahalu, D. Abush-Magder, U. Meirav, and M. A. Kastner, Nature (London) **391**, 156 (1988).
 - [6] S. M. Cronenwett, T. H. Oosterkamp, and L. P. Kouwenhoven, Science **281**, 540 (1998).
 - [7] D. Goldhaber-Gordon, J. Göres, M. A. Kastner, H. Shtrikman, D. Mahalu, and U. Meirav, Phys. Rev. Lett. **81**, 5225 (1998).
 - [8] L. P. Kouwenhoven, C. M. Marcus, P. L. McEuen, S. Tarucha, R. M. Westervelt, and N. S. Wingreen, in *Proceedings of the NATO Advanced Study Institute on Mesoscopic Electron Transport*, edited by L. L. Sohn, L. P. Kouwenhoven, and G. Schön (Kluwer, Dordrecht, 1997), p. E345.
 - [9] R. Hanson, L. P. Kouwenhoven, J. R. Petta, S. Tarucha, and L. M. K. Vandersypen, Rev. Mod. Phys. **79**, 1217 (2007).
 - [10] U. Gerland, J. von Delft, T. A. Costi, and Y. Oreg, Phys. Rev. Lett. **84**, 3710 (2000).
 - [11] P. Nozières, J. Low Temp. Phys. **17**, 31 (1974).
 - [12] M. Pustilnik and L. Glazman, J. Phys. Condens. Matter **16**, R513 (2004).
 - [13] P. G. Silvestrov and Y. Imry, Phys. Rev. Lett. **90**, 106602 (2003).
 - [14] G. Hackenbroich and H. A. Weidenmüller, Phys. Rev. Lett. **76**, 110 (1996).
 - [15] M. Avinun-Kalish, M. Heiblum, O. Zarchin, D. Mahalu, and V. Umansky, Nature (London) **436**, 529 (2005).
 - [16] Y. Ji, M. Heiblum, D. Sprinzak, D. Mahalu, and H. Shtrikman, Science **290**, 779 (2000).
 - [17] Y. Ji, M. Heiblum, and H. Shtrikman, Phys. Rev. Lett. **88**, 076601 (2002).
 - [18] M. Sato, H. Aikawa, K. Kobayashi, S. Katsumoto, and Y. Iye, Phys. Rev. Lett. **95**, 066801 (2005).
 - [19] G. Hackenbroich, Phys. Rep. **343**, 463 (2001).
 - [20] M. Ciorga, A. S. Sachrajda, P. Hawrylak, C. Gould, P. Zawadzki, S. Jullian, Y. Feng, and Z. Wasilewski, Phys. Rev. B **61**, R16315 (2000).
 - [21] A. Vidan, M. Stopa, R. M. Westervelt, M. Hanson, and A. C. Gossard, Phys. Rev. Lett. **96**, 156802 (2006).
 - [22] A. Yacoby, M. Heiblum, D. Mahalu, and H. Shtrikman, Phys. Rev. Lett. **74**, 4047 (1995).
 - [23] R. Schuster, E. Buks, M. Heiblum, D. Mahalu, V. Umansky, and H. Shtrikman, Nature (London) **385**, 417 (1997).
 - [24] D. Sprinzak, Y. Ji, M. Heiblum, D. Mahalu, and H. Shtrikman, Phys. Rev. Lett. **88**, 176805 (2002).
 - [25] J. König and Y. Gefen, Phys. Rev. B **65**, 045316 (2002).